Drug Design, Development and Therapy

Dovepress
open access to scientific and medical research

Open Access Full Text Article

ORIGINAL RESEARCH

A Gastric Cancer Peptide GX1-Modified Nano-Lipid Carriers Encapsulating Paclitaxel: Design and Evaluation of Anti-Tumor Activity

This article was published in the following Dove Press journal:
Drug Design, Development and Therapy

Drug Design, Development and Therapy downloaded from https://www.dovepress.com/
For personal use only.

Yufan Jian[1,2,*]
Meina Zhao[1,2,*]
Jinyi Cao[1,*]
Tingting Fan[1]
Wei Bu[1]
Yang Yang[3]
Weiwei Li[1]
Wei Zhang[1]
Yi Qiao[1]
Jingwen Wang[1]
Aidong Wen[1,2]

[1]Department of Pharmacy, Xijing Hospital, The Fourth Military Medical University, Xi'an 710032, People's Republic of China; [2]College of Pharmacy, Shannxi University of Chinese Medicine, Xianyang 712046, People's Republic of China; [3]Institute of Medical and Pharmaceutical Sciences, Zhengzhou University, Zhengzhou 450001, People's Republic of China

*These authors contributed equally to this work

Aim: The aim of this study was to develop a GX1-modified nanostructured lipid carrier (NLCs) and to evaluate its ability to improve the anti-gastric cancer tumor effects of paclitaxel (PTX).

Main Methods: The GX1-modified NLCs were synthesized and loaded with PTX (GX1-PTX-NLCs) by emulsion solvent evaporation technique. The anti-tumor activity and pharmacodynamics were then evaluated by in vitro cell studies and animal experiments.

Key Findings: The GX1-modified NLCs were successfully synthesized and confirmed by ^{1}H NMR and MALDI-TOF-MS. PTX-loaded NLCs produced particles with average size distribution less than or equal to 222 nm and good drug loading and entrapment efficiency. In vitro studies demonstrated that GX1-PTX-NLCs had a more obvious inhibitory effect on Co-HUVEC cells than PTX and unmodified PTX-NLCs. The cellular uptake results also showed that GX1-PTX-NLCs were largely concentrated in Co-HUVEC cells, and the uptake rates of GX1-PTX-NLCs in Co-HUVEC were higher than those of the free drug and the PTX-NLC. In vivo studies demonstrated that GX1-PTX-NLCs possess strong anti-tumor effect and showed higher tumor growth inhibition and lower toxicity in nude mice.

Significance: These results suggest that GX1-modified NLCs enhanced the anti-tumor activity of PTX and reduced its toxicity effectively. GX1-PTX-NLCs may be considered as a potent drug delivery system for therapy of gastric cancer.

Keywords: gastric cancer, paclitaxel, nano-lipid carriers, gastric cancer peptide, anti-tumor activity

Introduction

Gastric cancer (GC) ranks fourth in the incidence of malignant tumors worldwide[1–5] and is the second highest cause of cancer deaths.[6] Recently, the age of GC onset has reduced[7] while morbidity has increased.[8] Chemotherapy, the main treatment modality for GC exhibits poor therapeutic benefits and significant toxicity.[9,10] In fact, the five-year survival rate after comprehensive treatment has been estimated to be between 25~30%.[11,12] Within this context, new strategies able to treat malignant tumor, prolong survival period and improve quality of life are required to improve GC's therapeutic outcomes.

Targeted therapy, including tumor and tumor vasculature targeted therapy, has become popular due to excellent anti-tumor efficacy and low toxicity. Compared to tumor-targeted therapy, controlling tumor neovascularization is considered a more effective way to suppress tumor growth due to the dependence of tumor proliferation on angiogenesis.[13] Also, tumor vascular-targeted therapy is less prone to drug

Correspondence: Tingting Fan; Aidong Wen
Department of Pharmacy, Xijing Hospital, The Air Force Military Medical University, Xi'an 710032, People's Republic of China
Email fanting0427@163.com; adwen-2004@hotmail.com

submit your manuscript | www.dovepress.com
DovePress
http://doi.org/10.2147/DDDT.S233023

© 2020 Jian et al. This work is published and licensed by Dove Medical Press Limited. The full terms of this license are available at https://www.dovepress.com/terms.php and incorporate the Creative Commons Attribution – Non Commercial (unported, v3.0) License (http://creativecommons.org/licenses/by-nc/3.0/). By accessing the work you hereby accept the Terms. Non-commercial uses of the work are permitted without any further permission from Dove Medical Press Limited, provided the work is properly attributed. For permission for commercial use of this work, please see paragraphs 4.2 and 5 of our Terms (https://www.dovepress.com/terms.php).

resistance.[14] The key to vascular-targeted therapy is to find specific ligand molecules that target tumor blood vessels. By using in vivo screening of phage technology, a CGNSNPKSC (GX1) oligopeptide was identified as a ligand homing to receptors on human gastric adenocarcinoma vessel.[15,16] Previous studies have demonstrated that the GX1 peptide has good cell retention in U87MG cells and mainly targeted tumor vasculature in comparison to other organs.[17] GX1 has also been reported to enhance anti-tumor efficacy of nanomedicines. For instance, GX1-conjugated poly (lactic acid) nanoparticles encapsulating Endostar® significantly inhibited the growth of colorectal cancer tumors.[18] In another study, the inhibitory rate of GX1-modified liposomes carrying adenoviral vectors on GC vascular endothelial cells was 1.3 times more than those of adenovirus.[19] While GX1-modified docetaxel nanoparticles displayed good anti-tumor efficacy, it has low encapsulation efficiency and is unable to reduce the toxicity of docetaxel in vivo.[20]

Nanostructured lipid carriers (NLCs) are a new generation of low toxicity and good biocompatibility drug delivery systems developed from solid lipid nanoparticles (SLNs).[21–23] Perhaps their most important properties are their ability to facilitate higher drug loading.[24] Paclitaxel (PTX), a diterpenoid alkaloid, is a natural anticancer drug that is widely used in the treatment of GC.[25–29] However, due to gastrointestinal toxicity, allergies, cardiotoxicity, drug resistance and other side effects, the clinical application of PTX is limited.[30–33] Recently, in order to overcome some of PTX's defects, new dosage forms have been extensively studied using prodrugs,[34,35] liposomes,[36] and polymer nanoparticles.[37,38] However, several factors such as poor release rate, drug leakage, toxicity, high cost of raw material, drug resistance and unsatisfactory lipophilicity or bioavailability[39,40] have limited the clinical use of these dosage forms.[41]

In addition, although the PTX-loaded NLCs in publication have inhibitory ability on breast cancer cells, their anti-tumor effect in vivo is not clear,[42] and less attention has been paid to developing NLCs in treatment of GC. So based on these findings and problems, we prepared gastric cancer peptide GX1 mediated nanostructured lipid carriers loaded with PTX (Figure 1) and studied the anti-tumor activity of GX1-modified NLCs loaded with PTX (Figure 1) in gastric cancer. The NLCs were synthesized, modified with GX1 and fully characterized. PTX loading was accomplished by emulsion solvent evaporation. In vitro cell cytotoxicity, cellular inhibition and uptakes studies of the formulations were carried out and tumor-bearing nude mice was used to investigate the antitumor activity and side effect of GX1-PTX-NLCs in vivo.

Materials and Methods

Materials

PTX and 6-Hydroxycoumarin (6C) were obtained from Meilune Biotechnology Co., Ltd (Dalian, China). Stearic acid was received from Tianli Chemical Co., Ltd. (Tianjin, China). PEG2000 was from Kermel Chemical Co., Ltd. (Tianjin, China) and 4-dimethylaminopyridine (DMAP) from Fluorochem Co., Ltd. (Derbyshire, United Kingdom). Dicyclohexyl carbodiimide (DCC) was obtained from Acros Co., Ltd. (Belgium). Medium-chain triglyceride (MCT), triglyceride (TRIG) and Myrj 52 were obtained from RAM-M biotechnology Co., Ltd. (Nanjing, China). Solutol HS15 was obtained from Maya Reagent Co., Ltd. (Zhejiang, China). Succinic anhydride was obtained from Shanghai Fuchen Chemical Co., Ltd. (Shanghai, China). Pancreatin and high

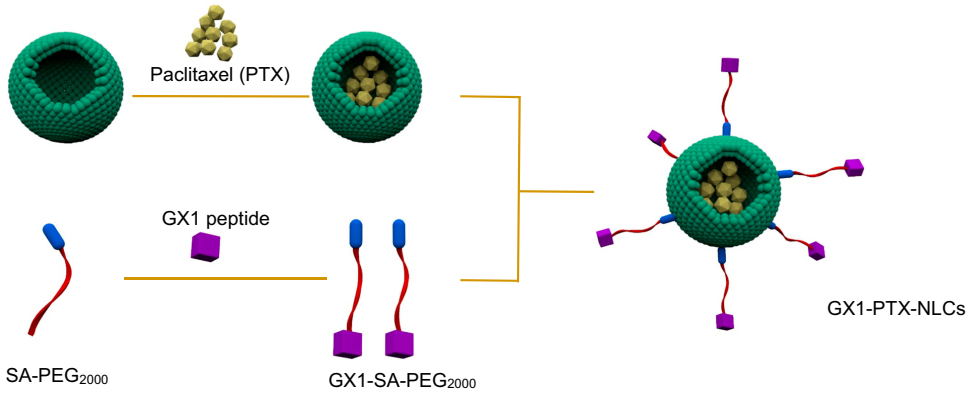

Figure 1 Schematic diagram of GX1-mediated drug targeting delivery system (GX1-PTX-NLCs).

glucose Dulbecco's Modified Eagle's Medium (DMEM) were purchased from GE biotechnology Co., Ltd. (USA). Penicillin streptomycin solution was received from Corning technology Co., Ltd. (New York, USA). Cell Counting Kit-8 was obtained from 7sea biotechnology Co., Ltd. (Shanghai, China). Fetal bovine serum (FBS) was received from Every green biotechnology Co., Ltd. (Hangzhou, China). Matrigel matrix was obtained from Becton, Dickinson and Company (BD) Co., Ltd. (USA).

HUVEC cell lines (Human umbilical vein endothelial cells; catalog number: C-12250) and GES-1 cell lines (immortalized fetal gastric mucosal cells) were obtained from the Institute of Biochemistry and Cell Biology (Shanghai, China), while MKN45 cells (Human gastric carcinoma cells) were obtained from Green biotechnology Co., Ltd. (Xi'an, China). Male BALB/C nude mice were supplied by the Vital River laboratory animal technology Co., Ltd. (Beijing, China).

Synthesis of SA-PEG2000-GX1

PEG2000-stearate (SA-PEG2000) was synthesized by slight modification of a previously reported method.[43] Briefly, stearic acid (SA, 1 mmol) was dissolved in 100 mL tetrahydrofuran (THF), followed by the addition of N, N-dicyclohexyl carbodiimide (DCC, 2.4 mmol) and 4-dimethylaminopyridine (DMAP, 0.1 mmol). The precipitated dicylcohexyl urea (DCU) was removed by filtration and the resulting filtrate was slowly dropped into a THF solution of polyethylene glycol 2000 (PEG2000, 2 mmol) maintained at 40°C. The reaction mixture was stirred at 40°C for 24 hrs and purified on a silica-gel chromatography column to obtain SA-PEG2000. In order to prepare SA-PEG2000-GX1, a carboxyl derivative of SA-PEG2000 was first synthesized by dissolving SA-PEG2000 (1 mmol) and succinic anhydride (1.5 mmol) in pyridine and reacting the mixture in an inert environment for 48 hrs at 80°C. Then, 10 mL HCl (2.8 mol/L) was added and the organic solvents removed. The SA-PEG2000-carboxyl derivative was then purified by column chromatography and confirmed by ^{1}H NMR. (BRUKER 400 MHz system, Karlsruhe, Germany, $CDCl_3$)

GX1 peptide was obtained by synthesizing linear nine peptide (3 mmol) on Wang resin using N,N'-Diisopropylcarbodiimide (DIC), 1-Hydroxybenzotriazole (HOBT) and DMAP as catalyst. For the looping of the peptide (GX1), I_2 and methanol were dropped into the reaction. SA-PEG2000-GX1 was then linked by adding O(7Azabenzotriazol1yl) NNN'N'tetramethyluronium hexafluorophosphate (HBTU) and N,N-Diisopropylethylamine (DIEA) to a mixture of GX1 (1 mmol) and SA-PEG2000-carboxyl derivative (1.5 mmol). SA-PEG2000-GX1 was verified by Matrix-Assisted Laser Desorption/Ionization Time of Flight Mass Spectrometry (MALDI-TOF-MS).

Preparation and Characterization of NLCs

Preparation of GX1-Bare-NLCs, PTX-NLCs and GX1-PTX-NLCs

The emulsion solvent evaporation method was used to prepare the NLCs[44] and the drug concentration was optimized based on previous reports.[45] Briefly, PTX (2mg), SA-PEG2000 (6mg), MCT (20mg) and TRIG (10mg) were dissolved in 3 mL of solvent (mixture of anhydrous ethanol and acetone at a volume ratio of 1:9) at 40°C. Subsequently, 10 mL Solutol HS 15 (1%, w/v) and Myrj 52 (1%, w/v) were added as surfactants. The emulsion was mixed by probe sonication at 160W for 2 min and the organic solvent evaporated under reduced pressure at 45°C to obtain the PTX-NLCs. For GX1-modified PTX-NLCs, SA-PEG2000 was replaced with SA-PEG2000-GX1, while GX1-modified blank NLCs (GX1-Bare-NLCs) were prepared in the same way as GX1-PTX-NLCs except for the addition of PTX.

Characterization of NLCs

The average particle size and zeta potential of PTX-NLCs and GX1-PTX-NLCs were determined using Beckman Coulter Delsa Nano C. The NLCs were first diluted with tri-distilled water and all measurements were carried out at 25±1°C, in triplicate.

Measurements of Entrapment Efficiency, Drug Loading and Formulation Stability

The entrapment efficiency (EE %) and drug loading capacity (DL %) of PTX-NLCs and GX1-PTX-NLCs were determined as previously reported.[46] Briefly, 0.1M HCl was added to the NLCs suspension and ultracentrifuged at 13,500 rpm for 30 min at 4°C. The concentration of drug in the supernatant and the amount of free drug were determined by HPLC. Furthermore, dispersions of NLCs were backing-dried at 100°C to obtain the total weight of NLCs. The EE % and the DL % of PTX-loaded NLCs were calculated by the equations given below:

$$EE\% = (\text{amount of PTX encapsulated in NLCs} / \text{initial amount of PTX}) \times 100\%$$

$$DL\% = \text{amount of PTX encapsulated in NLCs} / \text{total weight of NLCs} \times 100\%$$

To evaluate the stability of PTX-NLCs and GX1-PTX-NLCs, samples were collected after 4, 8, 12 and 16 days, followed by EE% and DL% determination. Furthermore, PTX-NLCs and GX1-PTX-NLCs suspensions were inspected for turbidity.

In vitro Drug Release Study

The in vitro drug release was determined by the dialysis bag method. Briefly, 2 mL each of PTX, PTX-NLCs and GX1-PTX-NLCs (PTX concentration of all samples was 80 μmol/L) was dissolved in PBS (pH 7.4) and put into a dialysis bag. The bag was then immersed in a dissolution medium (PBS; pH 7.4) and oscillated at a constant temperature (37±0.5°C, 100 rpm). At predetermined time intervals (0.5, 1, 2, 3, 4, 5, 8.10 and 15 hrs), 2 mL of the dissolution medium was collected and replaced with an equal amount of fresh PBS. The collected dissolution solutions were purified by filtration through a cellulose acetate membrane (0.45 μm) and the concentration determined by HPLC.

Cell Studies

Cell Culture

Co-HUVEC cells were used to simulate human gastric cancer vascular epithelial cells. HUVEC cells (1×10^6) and MKN45 cells (1×10^6) were seeded in the upper and the lower transwell chambers, respectively. The cells were maintained in DMEM supplemented with 10% FBS and 1% Penicillin streptomycin solution and incubated in a humidified atmosphere at 37°C in 5% CO_2. After 24 hrs, the Co-HUVEC cells were collected from the upper chambers.

Cytotoxicity Study and Cellular Inhibition Study

The Co-HUVEC and MKN45 cells were used for the cellular inhibition study, while HUVEC and GES-1 were used for the cytotoxicity study. CCK8 assay was used to assess cell viability. Briefly, the cells (2×10^3/well) were seeded into 96 well plates and incubated with PBS, PTX or NLCs suspensions (GX1-Bare-NLCs, PTX-NLCs and GX1-PTX-NLCs) at 37°C for 24 hrs. After 48 hrs, 10 μL of CCK8 reagent was added into each well and the plate was incubated for another 2 hrs in the dark conditions. Then, the absorbance of the solution was measured at 450 nm using a Varioskan® Flash spectral scanning multimode reader.

Cellular Uptake Study by Fluorescent Microscopy

A cell suspension of 1×10^5 cells/mL was seeded in 24 wells culture plates and incubated. After 24 hrs, the test substances (80 μmol/mL) were added to cells and incubated for 3 h. Subsequently, cells were fixed with 4% paraformaldehyde for 30 min, and then washed three times with PBS. DAPI solution was used to stain the nuclei and the specimens were observed using an Olympus fluorescent microscopy.

Quantitative Study of Cellular Uptake

A fluorescence dye (6-Hydroxycoumarin (6C)) was encapsulated in the NLCs for cell uptake study. Except for replacing PTX with 6C of equal mass (2mg), the preparation method of 6C-NLCs and GX1–6C-NLCs were the same as those of PTX-NLCs and GX1-PTX-NLCs. To observe intracellular uptake, the cells were plated at a density of 3×10^5 cells/well in 48-well plates and allowed to grow for 24 hrs. Then, the medium was replaced with 6C-PBS, 6C-NLCs or GX1–6C-NLCs and incubated for 3 h. Next, 0.5 mL of cell lysis solution was added to each well and the supernatant was obtained after centrifugation. Subsequently, fluorescence intensity of 6C was determined by fluorescence spectrophotometry and the protein content in cells was determined by BCA kit.

Animal Experiments

Tumor-Bearing Nude Mice Model

Forty-eight 5-week-old athymic nude mice were used to study the antitumor activity of the GX1-modified paclitaxel loaded NLCs. The MKN45 cells (5×10^6) were suspended with 0.2 mL PBS, mixed with equal volume matrigel matrix and injected subcutaneously into nude mice (BALB/c, nu/nu). The animals were kept in a pathogen-free environment with a 12 hr light/12 hr dark cycle, 50 ± 10% humidity, and 24 ± 2° C temperature. After 21 days, the tumor volumes of all nude mice were observed to be more than 70 mm^3. All experimental procedures were carried out according to protocols approved by the Ethics Committee for Animal Experimentation of the Fourth Military Medical University (Xi'an, Shaanxi, China) and were performed in accordance with the NIH Guide for the Care and Use of Laboratory Animals.

Evaluation of the Anti-Tumor Activity

Tumor-bearing nude mice were randomly divided into 4 groups (12 mice per group). Five doses of saline, free PTX (11.7 μmol/kg), PTX-NLCs (11.7 μmol/kg PTX equivalent)

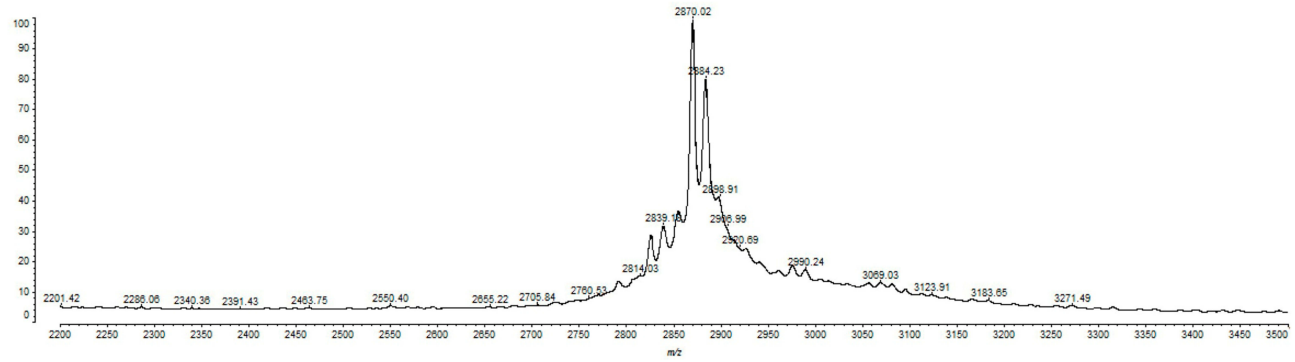

Figure 2 GX1-SA-PEG2000, MALDI-TOF-MS result.

or GX1-PTX-NLCs (11.7 μmol/kg PTX equivalent) were intravenously injected into tumor-bearing mice by tail vein every 3 days (1 d, 4 d, 7 d, 10 d and 13 d). Bodyweight of the mice was also monitored every 3 days as an indicator of systemic toxicity. To plot the tumor growth curve, the long (L) and short (W) diameter of the tumor were measured every 3 days with a caliper. The tumor volume was calculated as $LW^2/2$. On day 14, six mice in each group were euthanized and the tumor inhibition rate calculated. The remaining animals were left to observe the survival rate.

$$Tumor\ volume = 1/2 \times LW^2$$

$$Tumor\ inhibition\ rate(\%) = 1 - (Weight\ of\ treatment\ group / Weight\ of\ control\ group) \times 100\%$$

Tumor tissue of mice was immediately fixed with 4% neutral buffered formalin at 4°C overnight. Then, the fixed tissues were dehydrated and embedded in paraffin. Tissue sections (5 μm) were cut and stained by hematoxylin and eosin (H&E) for general histological examination. The tissue sections were observed under a Nikon microscope.

Results

Synthesis of SA-PEG$_{2000}$-GX1

SA-PEG2000 and SA-PEG$_{2000}$-GX1was successfully synthesized and confirmed by ^{1}H NMR and MALDI-TOF-MS. The structure of PEG2000-stearate (SA-PEG2000) was verified by ^{1}H NMR (see Supplemental Fig. S1)(^{1}H NMR, 400 MHz, CDCl3): (^{1}H-NMR, 400 MHz, CDCl3):δ4.18–4.14 (m, 2H), δ3.66–3.40 (m, 373H), δ2.28–2.23 (m, 3H), δ1.57–1.53 (m, 2H), δ1.22–1.18 (m, 26H), δ0.81 (t, J=6.8Hz, 3H). The structure of SA-PEG$_{2000}$-GX1 was confirmed by ^{1}H NMR (see Supplemental Fig. S2). (1H-NMR, 400 MHz, CDCl3):δ4.19–4.13 (m, 4H), δ3.67–3.40 (m, 350H), δ2.57–2.54 (m, 4H), δ2.29–2.24 (m, 2H), δ1.55–1.53 (m, 2H), δ1.21–1.18 (m, 26H), δ0.81 (t, J=6.8Hz, 3H); while that of SA-PEG$_{2000}$-GX1 was confirmed by MALDI-TOF-MS. MS (m/z):2870.02[M+Na]+ (Figure 2).

Preparation and Characteristics of PTX-NLCs and GX1-PTX-NLCs

The PTX-NLCs and GX1-PTX-NLCs were successfully prepared and characterized as shown in Table 1. The average particles size was below 222 nm with GX1-PTX-NLCs having larger particle sizes compared to PTX-NLCs. The zeta potential of GX1-PTX-NLCs decreased relative to PTX-NLCs probably due to the effect of the positively charged GX1 peptide. There was no difference (P>0.05) in the EE% between the two formulations. The particle shape observed under the transmission electron microscopy (TEM) were oval for both PTX-NLCs and GX1-PTX-NLCs. The observed size of the nanoparticles (TEM) was consistent with the measured average particles sizes (Figure 3). As shown in Figure 4, there was no change at 4°C in the particle size and EE% of PTX-loaded NLCs suspension within 12 days (P>0.05)

Table 1 Characterization of PTX-NLCs and GX1-PTX-NLCs

	Size/nm	Zeta Potential/mV	Entrapment Efficiency/%	Drug Loading Efficiency/%
PTX-NLCs	190.37 ± 3.78	−11.69 ± 0.40	80.63 ± 2.02	0.45 ± 0.017
GX1-PTX-NLCs	222.41 ± 2.02	−9.89 ± 0.37	80.16 ± 1.68	0.40 ± 0.013

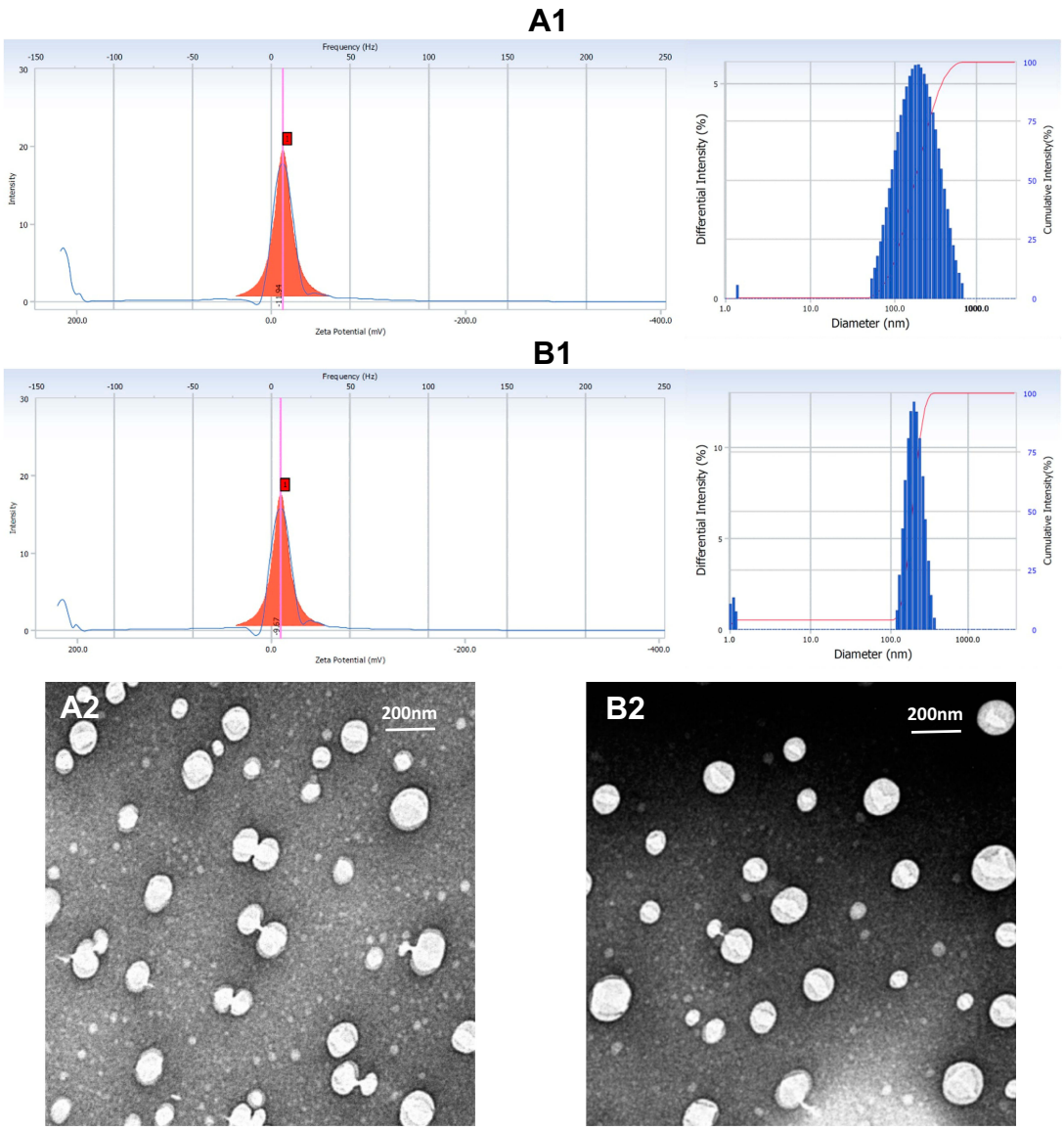

Figure 3 Mean zeta potential and particle size of PTX-NLCs (**A1**) and GX1-PTX-NLCs (**B1**). The morphology of two kinds of PTX-loaded NLCs. (**A2**) PTX-NLCs, (**B2**) GX1-PTX-NLCs.

indicating good stability. For GX1-PTX-NLCs, the particle sizes observed after 8 days were larger than those of the original dispersion, indicating that samples became unstable after 8 days. For all the samples evaluated, the nanoparticle solutions were clear and transparent, and there was no change in EE% up to 16 days.

In vitro Drug Release Study

The ability of NLCs to deliver PTX was examined by monitoring the drug release. As shown in Figure 5, the release rate of free PTX solution was nearly 80% after 2 hrs, with the drug almost completely released at 4 hrs. The percentage of drug burst release from PTX-NLCs and GX1-PTX-NLCs were 50.31% and 47.24% after 2 hrs, respectively. In addition, the release rate of GX1-PTX-NLCs increased slightly after 5 hrs compared with that of PTX-NLCs. The amounts of PTX released from the two NLCs formulations were 100% after 14 hrs, whereas about 100% of the free drug was found in dissolution medium after approximately 4 hrs.

Cell Studies

Cytotoxicity Study

The cytotoxicity of PTX, GX1-Bare-NLCs, PTX-NLCs and GX1-PTX-NLCs was evaluated by CCK8 assay. As shown in Figure 6A, the cytotoxicity of GX1-PTX-NLCs on HUVEC cells was significantly lower than that of PTX, while the inhibition rate of PTX-NLCs on HUVEC cells was the lowest. The inhibitory effects of the PTX and NLCs on GES-1 were in

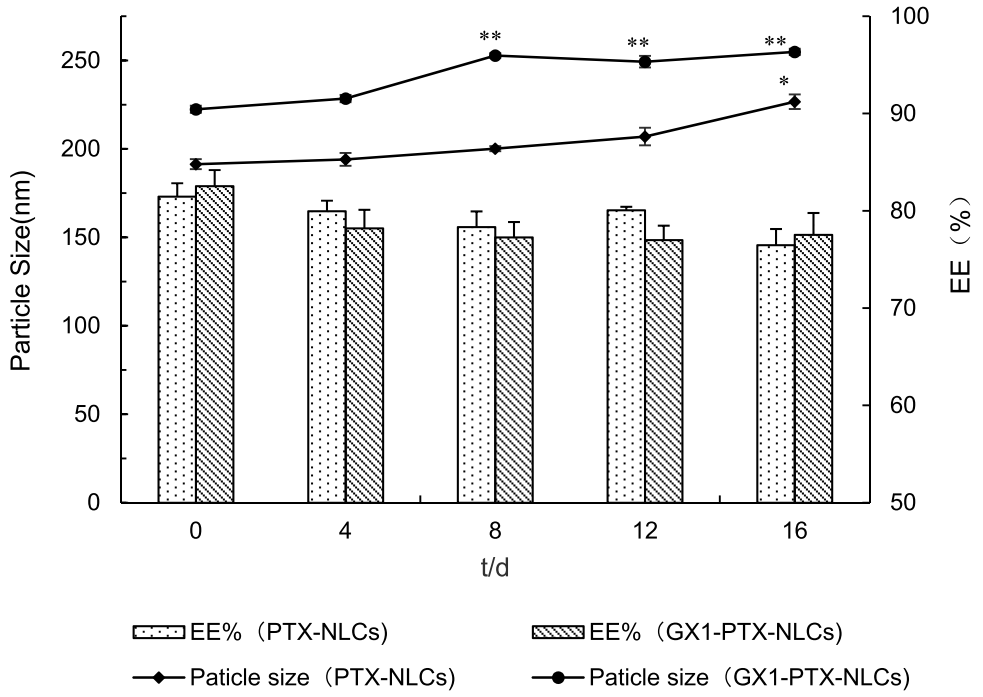

Figure 4 The stability experiment result of two kinds of paclitaxel nanoparticles within 16 days (n=3, **P<0.01).

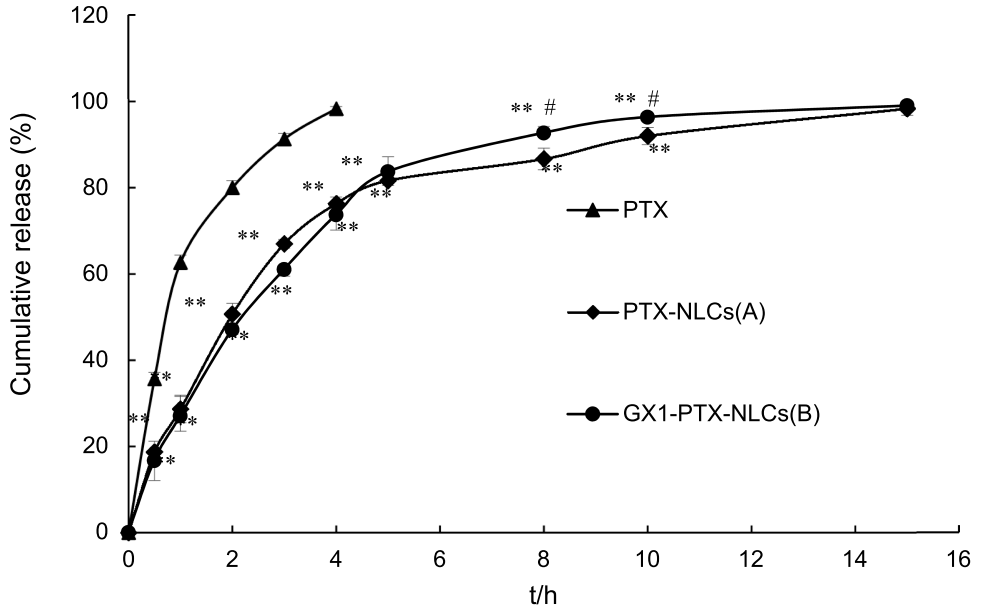

Figure 5 In vitro release curves of paclitaxel, PTX-NLCs (**A**) and GX1-PTX-NLCs (**B**) in PH 7.4 PBS (n=3). Significant difference between two kinds of NLCs and free PTX ($^{\#}$p<0.05, **P<0.01).

the following order: GX1-PTX-NLCs < PTX-NLCs < PTX. GES-1. The cells in GX1-PTX-NLCs group showed the highest survival rate (81.45±0.64%). Also, the observed difference between GX1-Bare-NLCs and GX1-PTX-NLCs demonstrated the ability of GX1 reduced the toxicity of nanoparticles to GES-1 cells.

Cellular Inhibition Study

As can be seen from Figure 6B, GX1-PTX-NLCs showed a more obvious inhibitory effect on Co-HUVEC cells than PTX and PTX-NLCs. It is concluded that GX1, a vascular targeting peptide, can inhibit the growth of Co-HUVEC. All nanoparticles had the strong inhibitory effect on MKN45

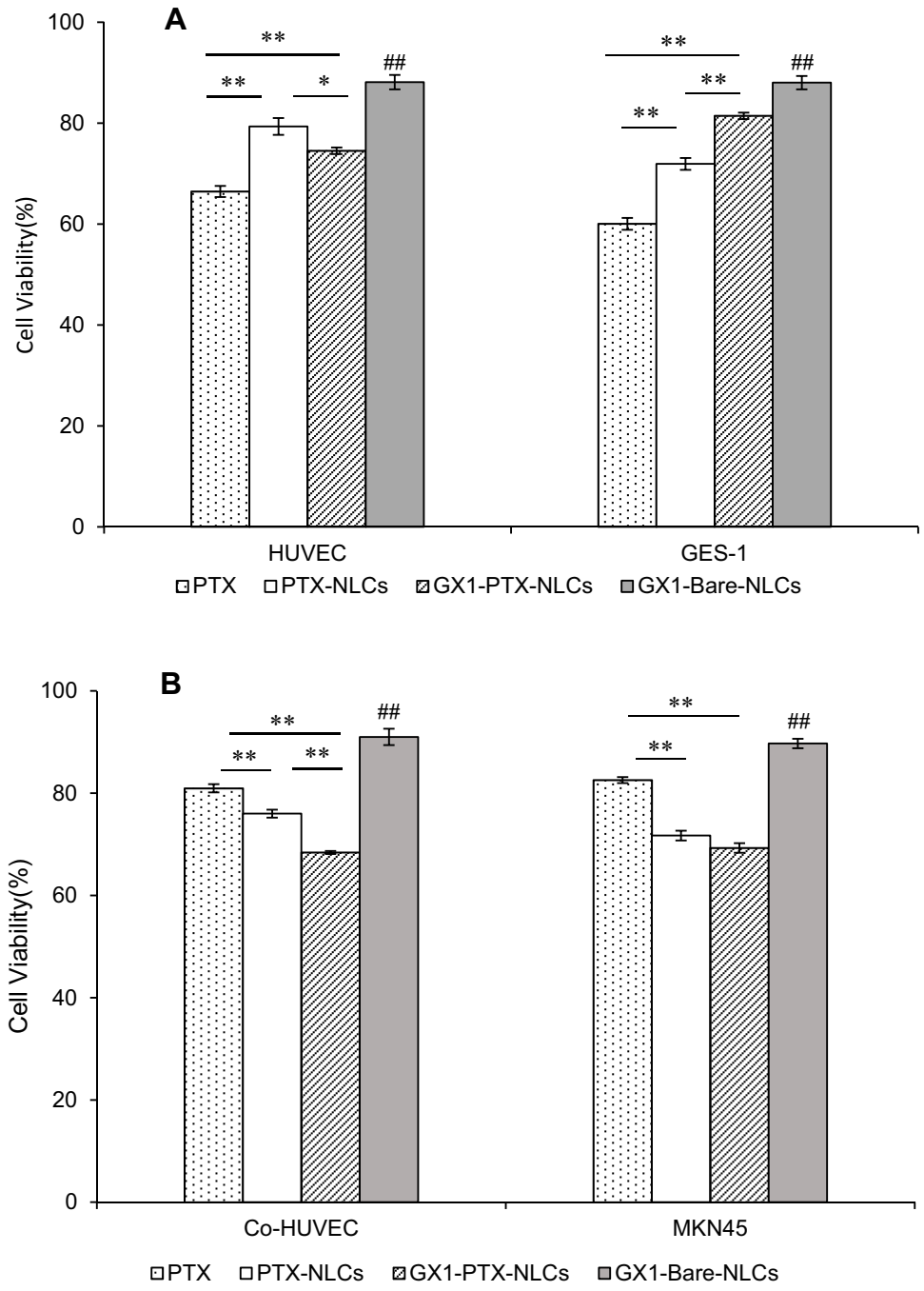

Figure 6 The cytotoxicity (**A**) and growth-inhibitory effect (**B**) of PTX, PTX-NLCs and GX1-PTX-NLCs on various cells for 24 hrs. GX1-PTX-NLCs showed the most inhibitory effect on Co-HUVEC cells. All Nano-lipid carriers had the strong inhibitory effect on MKN45 cells (n=3, #GX1-Bare-NLCs VS PTX/PTX-NLCs/GX1-PTX-NLCs, $^{\#\#}P<0.01$, $^{**}P<0.01$).

cells. In comparison to PTX-NLCs (27.44±0.59%), GX1-PTX-NLCs did not produce a significantly higher effect on MKN45 cells (28.70±0.94%). Meanwhile, the inhibition rate of the blank lipid carriers on Co-HUVEC and MKN45 cells were only 9% and 11%, respectively.

Cellular Uptake Study by Fluorescent Microscopy

The distribution of 6C, 6C-NLCs and GX1–6C-NLCs was observed under fluorescence microscope. As shown in Figure 7A, only a small number of 6C molecules entered MKN45 cells while the two NLCs aggregated in a large

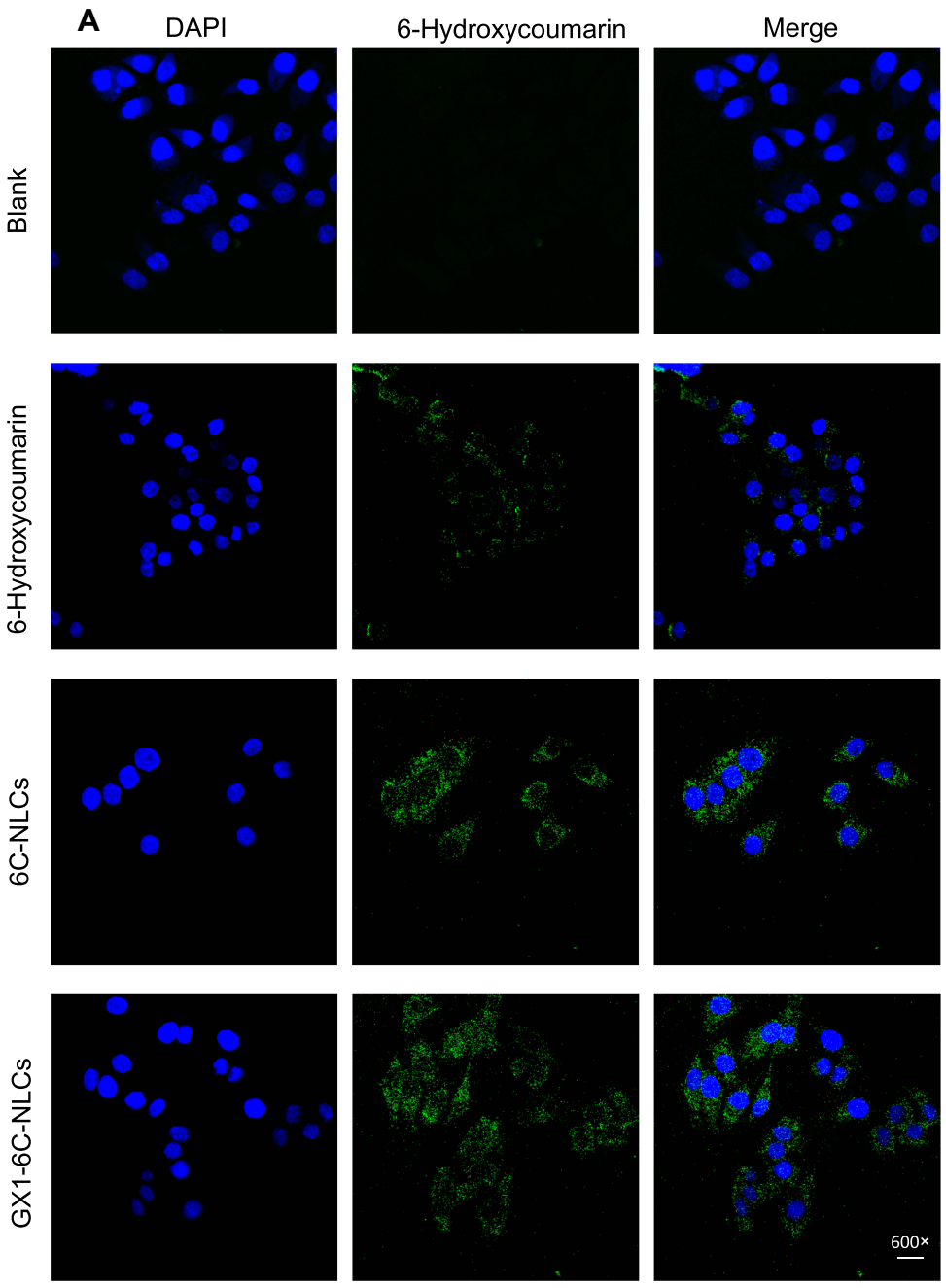

Figure 7 Continued.

number of tumor cells. In Co-HUVEC cells, GX1-modified 6C nanoparticles produced stronger storage capacity than non-modified 6C nanoparticles. The fluorescence intensity of the two nanoparticles in Co-HUVEC was significantly higher than in the group treated with free 6C (Figure 7B). The results showed that both NLCs increased the concentration of PTX in MKN45, while only GX1-modified NLC could enhance the ability of PTX to enter Co-HUVEC cells.

Quantitative Study of Cellular Uptake

The quantitative intracellular uptake was investigated by BCA protein assay. As shown in Figure 8, a larger amount of 6C in GX1–6C-NLCs was taken up by Co-HUVEC cells (85.26±0.52%), while the uptake rates of free 6C and 6C-NLCs in Co-HUVEC cells were 76.21 ±0.32% and 71.82±0.65%, respectively. This indicated that 6C in the two NLCs easily accumulated in Co-

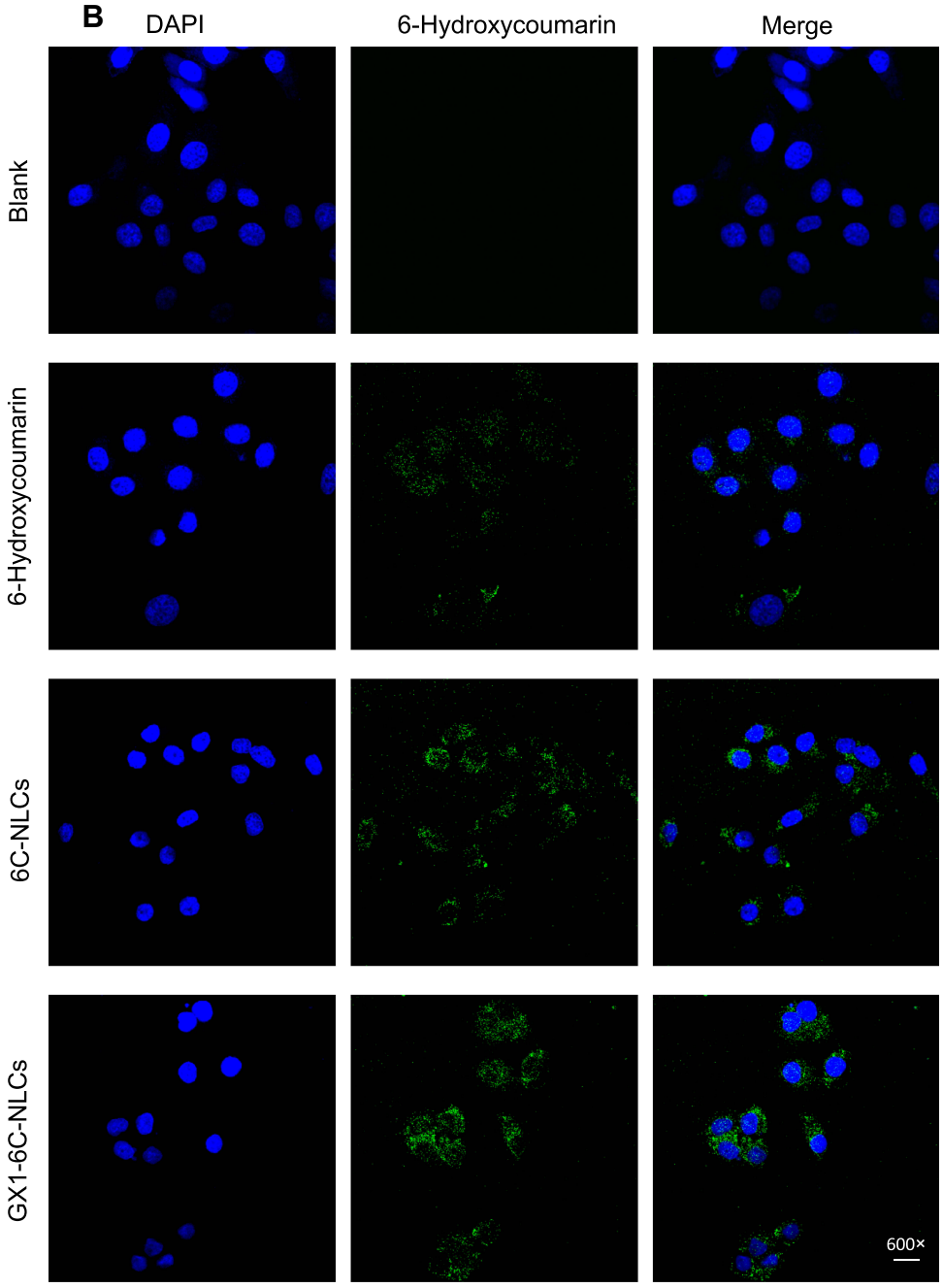

Figure 7 Intracellular localization of 6-Hydroxycoumarin, 6C-NLCs and GX1–6C-NLCs. From left to right, there were images of DAPI staining for nucleus (blue dots), 6-Hydroxycoumarin (green dots) and their merged images. (**A**). MKN45 cells were treated with 80 nmol/mL of 6C, 6C-NLCs and GX1–6C-NLCs for 30 min, respectively. Both two NLCs increased the concentration of PTX in MKN45. (**B**). Co-HUVEC cells were treated with 80 nmol/mL of 6C, 6C-NLCs and GX1–6C-NLCs for 30 min, respectively. GX1–6C-NLCs have stronger storage capacity than PTX and PTX-NLCs. The scale bar represents 10 μm.

HUVEC cells compared to free 6C. In addition, compared to free 6C, the two NLCs had a higher uptake rate MKN45 cells, but there was no significant difference in the uptake rates between 6C-NLCs (90.22 ±0.67%) and GX1–6C-NLCs (88.00±1.97%).

Animal Experiments

Efficacy Evaluation of the Three Drugs on Nude Mice

The growth curve of the tumors is shown in Figure 9A. When used at the dosage of 10 mg/kg, the three drugs can inhibit tumor growth after 4, 7, 10 and 13 days. The anti-tumor

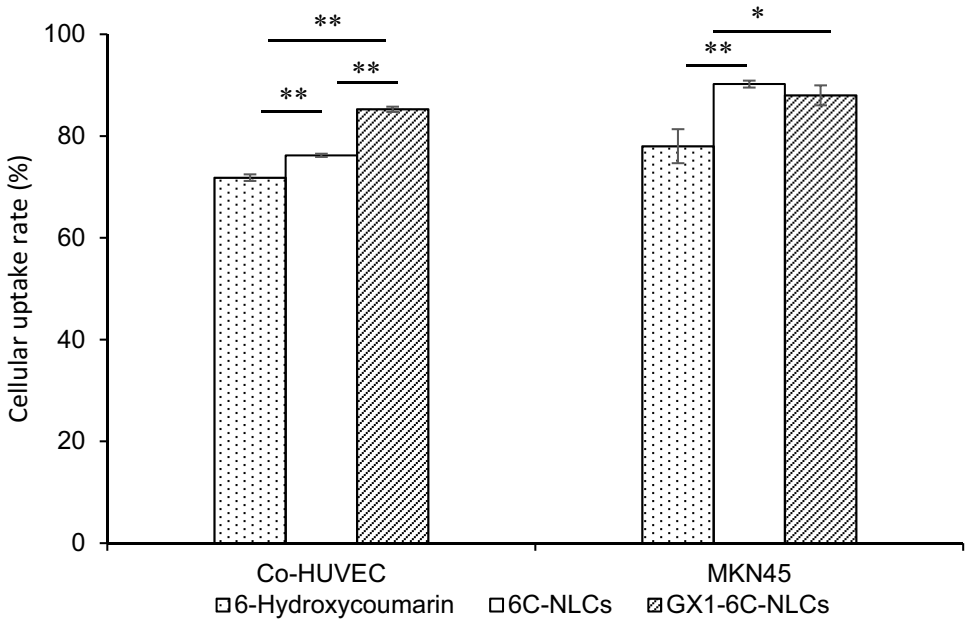

Figure 8 Cellular uptake of 6-Hydroxycoumarin, 6C-NLCs and GX1–6C-NLCs on MKN45 cells and Co-HUVEC cells for 3 hrs. Co-HUVEC cells had a higher uptake rate of GX1–6C-NLCs (n = 3, *P<0.05, **P<0.01).

effect of PTX was weaker than those of the NLCs. When compared, it was found that the anti-tumor activity of GX1-PTX-NLCs was better than that of PTX-NLCs (**P < 0.01). After 14 days, six mice in each group were sacrificed. The results showed that the tumor volume of model group was 704.72±29.59mm^3, while that of the GX1-PTX-NLCs group was 373.27±16.32mm^3. The inhibition rate after 14d was found to be 69.70±4.37% and 29.11±5.07% for the GX1-PTX-NLCs and PTX respectively (Table. 2). The exfoliated tumor is shown in Figure 9B.

The change in bodyweight is one of the important indexes to evaluate the toxic and side effects of drugs. Figure 9C shows that the bodyweight of mice in GX1-PTX-NLCs and PTX-NLCs groups did not produce any significant change within 14 days (P > 0.05), while that of other groups decreased. The bodyweight of mice in model group decreased significantly from 4 days, and that of PTX decreased more obviously after 7 days. The data suggest that the toxicity of the two NLCs to nude mice was less than that of PTX. In addition, treatment with two NLCs also prolonged the survival time of mice. After 22 days, all the mice in control group died. Only one in PTX group survived at 30 days, indicating that PTX had therapeutic effect but with toxic side effects. In contrast, there were no death in two NLCs groups after 30 days of treatment. Notably, GX1-PTX-NLCs prolonged the survival time of tumor-bearing nude mice to 44 days, indicating that two NLCs could Inhibit tumor growth without no serious adverse effects (Figure 9D).

Histopathological Analysis

The histological characteristics of the tumors were evaluated by hematoxylin-eosin staining. As shown in Figure 10, MKN45 cells in nude mice of model group had distinct morphology, clear nuclear staining and complete cell morphology, indicating that the tumor tissue was in the state of growth or proliferation. In PTX treatment

Table 2 The Tumor Inhibition Rate of Each Group

Group	Tumor Weight							Inhibition Rate (%)
	1	2	3	4	5	6	X ± S	
Con	1.59	1.41	1.47	1.49	1.56	1.44	1.49 ± 0.07	0
PTX	1.09	1.04	1.13	1.08	0.97	1.03	1.06 ± 0.06	29.11 ± 5.07
PTX-NLCs	0.74	0.71	0.66	0.79	0.68	0.72	0.72 ± 0.05	51.93 ± 3.63
GX1-PTX-NLCs	0.41	0.39	0.56	0.42	0.47	0.46	0.45 ± 0.06	69.70 ± 4.37

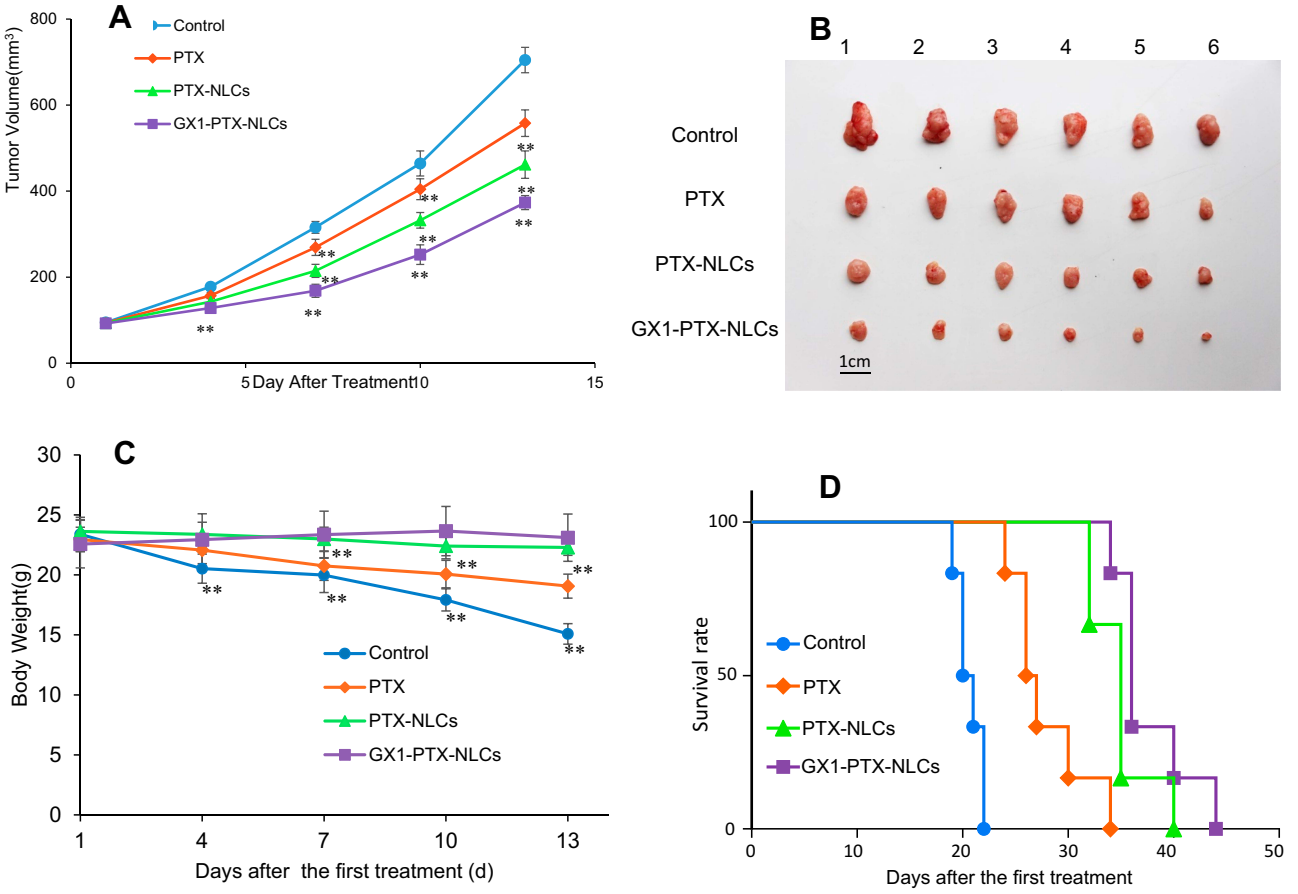

Figure 9 Inhibition of tumor growth in nude mice. (**A**) The tumor size was measured every three days and the volume were calculated. Significant difference size between each group. (**B**) Tumors exfoliated from animals after 14 days treatment. (**C**) The body weight change in different group, the bodyweight of mice in GX1-PTX-NLCs and PTX-NLCs groups had no significant difference within 14 days (n=6). (**D**) The survival curve of nude mice with tumors, GX1-PTX-NLCs could prolong the survival time of tumor-bearing nude mice (n=6, **P<0.01).

group, the cell size was not uniform, and some cells showed necrosis. The morphology of the cells in the nanoparticles group was blurred and a large number of cell fragments were observed suggesting that cell necrosis in the tissues. In GX1-PTX-NLCs group, cell shrinkage was obvious, and necrosis appeared in large area of the tissues (Arrow marked).

Discussion

In this study, we developed a novel GX1-modified NLCs delivery system encapsulating PTX. Because the cell membrane is a bilayer structure of phospholipids, lipid carriers are easily absorbed by cells with minimal adverse reactions. It has been reported that[47] in lipid carriers, peptide ligands can be linked to phospholipids such as 1,2-bisstearoyl phosphatidylethanolamine (DSPE). Compared with DSPE, stearic acid has the advantages of high chemical stability and low cost.

Emulsified solvent evaporation is a common method to prepare nanoparticles. In this study, lipid nanoparticles were homogenized by ultrasonic cell grinder and the average particle size distribution was about 160 ~ 240 nm. It is worth mentioning that particle size of GX1-PTX-NLCs was much larger than that of PTX-NLCs. It is possible that the surface GX1 peptide extension of NLCs made their particle size larger. In the stability experiments, there was no significant difference in EE of PTX-NLCs up to 16d. The average particle size of GX1-PTX-NLCs began to increase at 8d ~ 16d, indicating loss of stability probably due to smaller zeta potential of GX1-PTX-NLCs relative to PTX-NLCs. However, the EE of GX1-PTX-NLCs was not influenced.

MKN45 cells have been widely used as tumor cells for gastric cancer studies.[48,49] The effect of free PTX and the two NLCs on the inhibition of tumor cells and cytotoxicity of healthy cells were investigated by CCK8 assay. It was found that GX1-PTX-NLCs had the strongest inhibitory effect (higher than that of PTX-NLCs and PTX) on Co-HUVEC cells when the concentration of PTX was 80

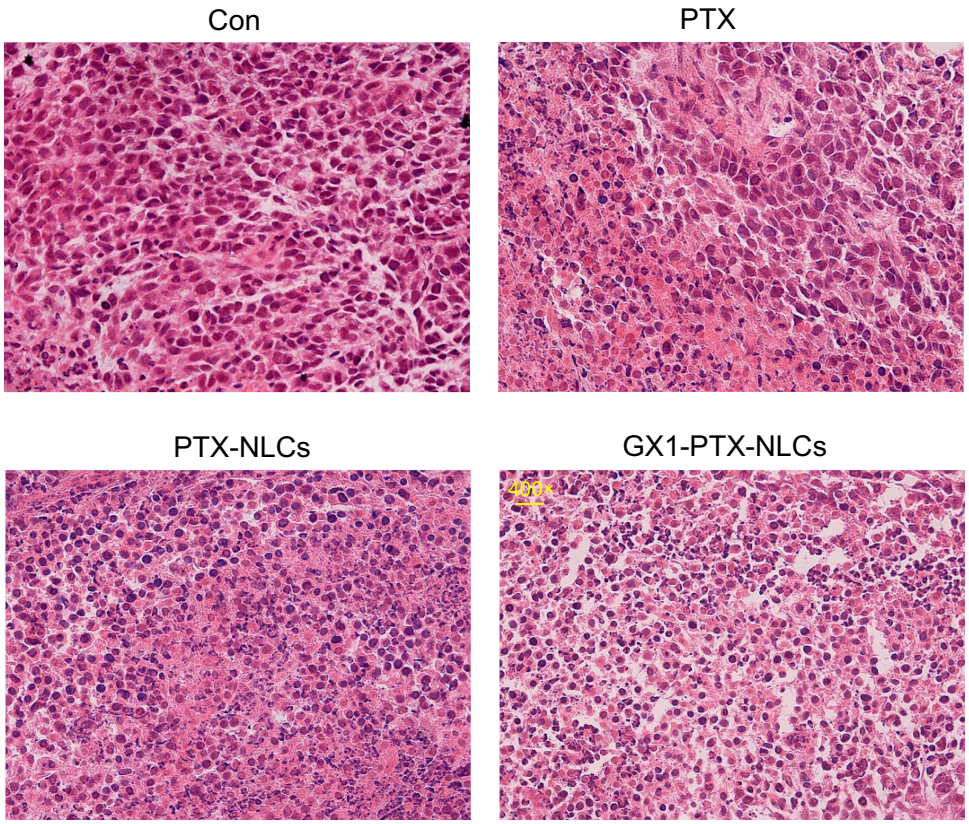

Figure 10 H&E staining for histological examination (upper panel). Cell shrinkage was obvious, and necrosis appeared in large area of the tissues in GX1-PTX-NLCs group. Data are a typical microscopic imaging of tumor tissue sections under original magnification of × 400. H&E Nuclei: blue, cytoplasm: pink. The scale bar represents 20 μm.

μmol/mL. This suggests that GX1 could effectively inhibit the growth of vascular endothelial cells of gastric cancer. Also, the inhibition rate of GX1-PTX-NLCs on MKN45 cells was lower than that of PTX-NLCs. The receptors of GX1 are mainly distributed in gastric adenocarcinoma vessel, but rarely in MKN45 cells[16] thereby resulting in GX1-PTX-NLCs poor ability to target MKN45 cells. It can be seen from the toxicity experiments that the cytotoxicity of the two NLCs on GES-1 cells were less than that of PTX, while the cytotoxicity of GX1-PTX-NLCs was less than that of PTX-NLCs. Because GX1 can specifically target and bind to HUVEC cells,[50] GX1-PTX-NLCs produced a stronger cytotoxic effect on HUVEC cells relative to PTX-NLCs. These data demonstrated that the cytotoxicity of PTX against healthy cells could be reduced by incorporating it into NLCs.

In order to further observe the cellular uptake of GX1-modified nanoparticles on MKN45 and Co-HUVEC cells, NLCs containing 6C instead of PTX were prepared.[51] The results showed that the uptake rates of the PTX and the two NLCs by Co-HUVEC cells were in the order of GX1–6C-NLCs > 6C-NLCs > free 6C, while the GX1–6C-NLCs and 6C-NLCs had no significant difference uptake effect on MKN45. The results of the cellular uptake study were consistent with those from the CCK8 assay, indicating that GX1 can increase the selective adsorption ability of nanoparticles to Co-HUVEC cells.

A nude mouse model of human gastric cancer was established. The results showed that there were significant differences in the size of tumors in each group from the fourth day of administration. Compared with PTX-NLCs (51.93% ±3.63) and PTX (29.11%±5.07), the growth of tumors in GX1-PTX-NLCs group was significantly inhibited (69.70% ±4.37). The data indicates that GX1-PTX-NLCs improves tumor growth inhibition. Hematoxylin and eosin staining results also showed that tumor tissue in PTX group had partial necrosis, while those of the NLC groups had large area of necrosis. Combining the results of CCK8 assay and cellular uptake study, it could be concluded that GX1-PTX-NLCs showed a better effect on suppressing tumor growth. Bodyweight change is one of the useful indicators for evaluating toxicity.[52] After 14 days, the weight of BALB/C nude mice treated with NLCs did not change significantly. Conversely, those in PTX group lost 14% of their body

weight. Furthermore, GX1-PTX-NLCs prolonged the survival time of the animals more than PTX. Overall, the in vivo experiments indicate that the drug carrier modified with GX1 not only enhanced the anti-tumor effect of PTX but also greatly reduced the toxic side effects of the drug.

This study focused on the anti-tumor effect of GX1-PTX-NLCs and did not explore the targeting of GX1-mediated NLC in depth. Moreover, to further evaluate the necrosis degree of tumor tissues, immunohistochemistry assay involving vascular marker like CD31 will be included in future research.

Conclusion

GX1-modified NLCs were successfully synthesized and loaded with PTX. The NLC formulations showed good entrapment efficiency, drug loading and particle characteristics. The in vitro study indicated that GX1 modification of NLCs enhanced uptake of PTX by Co-HUVEC cells. In addition, the cytotoxicity of GX1-PTX-NLCs was minimal on GES-1 cells. Compared with PTX and PTX-NLCs, the tumor growth of nude mice was significantly inhibited by GX1-PTX-NLCs. Results of weight of nude mice suggest that the side effects of the two kinds of nanoparticles on nude mice were less than that of PTX. The data above indicate the gastric cancer vasculature targeted peptide GX1-modified NLC loaded with PTX is a potentially effective formulation or gastric cancer therapy.

Acknowledgments

The authors acknowledge the financial assistance of this research from the Natural Science Foundation of China [Grant # 81602640] [Grant # 81602720].

Author Contributions

All authors contributed to data analysis, drafting or revising the article, gave final approval of the version to be published, and agree to be accountable for all aspects of the work.

Disclosure

The authors report no conflicts of interest in this work.

References

1. Siegel RL, Miller KD, Jemal A. Cancer statistics. *CA Cancer J Clin*. 2017;67(1):7–30. doi:10.3322/caac.21387
2. Digklia A, Wagner AD. Advanced gastric cancer: current treatment landscape and future perspectives. *World J Gastroenterol*. 2016;22(8):2403–2414. doi:10.3748/wjg.v22.i8.2403
3. Oh SC. Update of adjuvant chemotherapy for resected gastric cancer. *J Gastric Cancer*. 2012;12(1):3–6. doi:10.5230/jgc.2012.12.1.3
4. Schwarz RE, Smith DD. Clinical impact of lymphadenectomy extent in resectable gastric cancer of advanced stage. *Ann Surg Oncol*. 2007;14(2):317–328. doi:10.1245/s10434-006-9218-2
5. Jemal A, Bray F, Center MM, Ferlay J, Ward E, Forman D. Global cancer statistics. *CA Cancer J Clin*. 2011;61(2):69–90. doi:10.3322/caac.20107
6. Chen W, Zheng R, Baade PD, et al. Cancer statistics in China, 2015. *CA Cancer J Clin*. 2016;66(2):115–132. doi:10.3322/caac.21338
7. Maden CH, Gomes J, Schwarz Q, Davidson K, Tinker A, Ruhrberg C. NRP1 and NRP2 cooperate to regulate gangliogenesis, axon guidance and target innervation in the sympathetic nervous system. *Dev Biol*. 2012;369(2):277–285. doi:10.1016/j.ydbio.2012.06.026
8. Nishikawa K, Aoyama T, Oba MS, et al. The clinical impact of Hangeshashinto (TJ-14) in the treatment of chemotherapy-induced oral mucositis in gastric cancer and colorectal cancer: analyses of pooled data from two Phase II randomized clinical trials (HANGESHA-G and HANGESHA-C). *J Cancer*. 2018;9(10):1725–1730. doi:10.7150/jca.24733
9. Lee JH, Kim JG, Jung HK, et al. Clinical practice guidelines for gastric cancer in Korea: an evidence-based approach. *J Gastric Cancer*. 2014;14(2):87–104. doi:10.5230/jgc.2014.14.2.87
10. Xin J, Wang S, Wang B, et al. AlPcS4-PDT for gastric cancer therapy using gold nanorod, cationic liposome, and Pluronic((R)) F127 nanomicellar drug carriers. *Int J Nanomed*. 2018;13:2017–2036. doi:10.2147/IJN.S154054
11. Kim HS, Kim JH, Kim JW, Kim BC. Chemotherapy in elderly patients with gastric cancer. *J Cancer*. 2016;7(1):88–94. doi:10.7150/jca.13248
12. Farran B, Muller S, Montenegro RC. Gastric cancer management: kinases as a target therapy. *Clin Exp Pharmacol Physiol*. 2017;44(6):613–622. doi:10.1111/1440-1681.12743
13. Folkman J. Tumor angiogenesis: therapeutic implications. *N Engl J Med*. 1971;285(21):1182–1186. doi:10.1056/NEJM197111182852108
14. Yang T, Wang Y, Li Z, et al. Targeted delivery of a combination therapy consisting of combretastatin A4 and low-dose doxorubicin against tumor neovasculature. *Nanomedicine*. 2012;8(1):81–92. doi:10.1016/j.nano.2011.05.003
15. Zhi M, Wu KC, Dong L, et al. Characterization of a specific phage-displayed peptide binding to vasculature of human gastric cancer. *Cancer Biol Ther*. 2004;3(12):1232–1235. doi:10.4161/cbt.3.12.1223
16. Hui X, Han Y, Liang S, et al. Specific targeting of the vasculature of gastric cancer by a new tumor-homing peptide CGNSNPKSC. *J Control Release*. 2008;131(2):86–93. doi:10.1016/j.jconrel.2008.07.024
17. Chen K, Sun X, Niu G, et al. Evaluation of 64Cu labeled GX1: a phage display peptide probe for PET imaging of tumor vasculature. *Mol Imaging Biol*. 2012;14(1):96–105. doi:10.1007/s11307-011-0479-1
18. Du Y, Zhang Q, Jing L, et al. GX1-conjugated poly(lactic acid) nanoparticles encapsulating endostar for improved in vivo anticolorectal cancer treatment. *Int J Nanomed*. 2015;10:3791–3802. doi:10.2147/IJN.S82029
19. Xiong D, Liu Z, Bian T, et al. GX1-mediated anionic liposomes carrying adenoviral vectors for enhanced inhibition of gastric cancer vascular endothelial cells. *Int J Pharm*. 2015;496(2):699–708. doi:10.1016/j.ijpharm.2015.11.019
20. Zhang E, Xing R, Liu S, et al. Vascular targeted chitosan-derived nanoparticles as docetaxel carriers for gastric cancer therapy. *Int J Biol Macromol*. 2019;126:662–672. doi:10.1016/j.ijbiomac.2018.12.262
21. Raza K, Shareef MA, Singal P, Sharma G, Negi P, Katare OP. Lipid-based capsaicin-loaded nano-colloidal biocompatible topical carriers with enhanced analgesic potential and decreased dermal irritation. *J Liposome Res*. 2014;24(4):290–296. doi:10.3109/08982104.2014.911314

22. Kamaly N, Xiao Z, Valencia PM, Radovic-Moreno AF, Farokhzad OC. Targeted polymeric therapeutic nanoparticles: design Development and Clinical Translation. *Chem Soc Rev*. 2012;41(7):2971–3010.
23. Bareschino MA, Schettino C, Rossi A, et al. Treatment of advanced non small cell lung cancer. *J Thorac Dis*. 2011;3(2):122–133. doi:10.3978/j.issn.2072-1439.2010.12.08
24. Chen CC, Tsai TH, Huang ZR, Fang JY. Effects of lipophilic emulsifiers on the oral administration of lovastatin from nanostructured lipid carriers: physicochemical characterization and pharmacokinetics. *Eur J Pharm Biopharm*. 2010;74(3):474–482. doi:10.1016/j.ejpb.2009.12.008
25. Ryu MH, Ryoo BY, Kim TW, et al. A phase I/IIa study of DHP107, a novel oral paclitaxel formulation, in patients with advanced solid tumors or gastric cancer. *Oncologist*. 2017;22(2):129–e8. doi:10.1634/theoncologist.2016-0273
26. Qian J, Qian Y, Wang J, et al. A clinical prognostic scoring system for resectable gastric cancer to predict survival and benefit from paclitaxel- or oxaliplatin-based adjuvant chemotherapy. *Drug Des Devel Ther*. 2016;10:241–258. doi:10.2147/DDDT.S88743
27. Wang SQ, Wang C, Chang LM, et al. Geridonin and paclitaxel act synergistically to inhibit the proliferation of gastric cancer cells through ROS-mediated regulation of the PTEN/PI3K/Akt pathway. *Oncotarget*. 2016;7(45):72990–73002. doi:10.18632/oncotarget.12166
28. Sasaki Y, Nishina T, Yasui H, et al. Phase II trial of nanoparticle albumin-bound paclitaxel as second-line chemotherapy for unresectable or recurrent gastric cancer. *Cancer Sci*. 2014;105(7):812–817. doi:10.1111/cas.12419
29. Zhang C, Awasthi N, Schwarz MA, Hinz S, Schwarz RE. Superior antitumor activity of nanoparticle albumin-bound paclitaxel in experimental gastric cancer. *PLoS One*. 2013;8(2):e58037. doi:10.1371/journal.pone.0058037
30. Ozcelik B, Turkyilmaz C, Ozgun MT, et al. Prevention of paclitaxel and cisplatin induced ovarian damage in rats by a gonadotropin-releasing hormone agonist. *Fertil Steril*. 2010;93(5):1609–1614. doi:10.1016/j.fertnstert.2009.02.054
31. Barbuti AM, Chen ZS. paclitaxel through the ages of anticancer therapy: exploring its role in chemoresistance and radiation therapy. *Cancers*. 2015;7(4):2360–2371. doi:10.3390/cancers7040897
32. Sonnenblick A, Eleyan F, Peretz T, et al. Gemcitabine in combination with paclitaxel for advanced soft-tissue sarcomas. *Mol Clin Oncol*. 2015;3(4):829–832. doi:10.3892/mco.2015.545
33. Neijt JP, Engelholm SA, Tuxen MK, et al. Exploratory Phase III study of paclitaxel and cisplatin versus paclitaxel and carboplatin in advanced ovarian cancer. *J Clin Oncol*. 2000;18(17):3084–3092. doi:10.1200/JCO.2000.18.17.3084
34. Mao Y, Zhang Y, Luo Z, et al. Synthesis, biological evaluation and low-toxic formulation development of glycosylated paclitaxel prodrugs. *Molecules*. 2018;23(12):3211. doi:10.3390/molecules23123211
35. Ding Y, Jia Y, Lu C, et al. In vitro assessment of cytochrome P450 inhibition and induction potential of felotaxel (SHR110008). *Biomed Pharmacother*. 2012;66(4):318–321. doi:10.1016/j.biopha.2012.01.001
36. Zhou L, Luo W. Vascular endothelial growth factor-targeted paclitaxel-loaded liposome microbubbles and inhibition of human epidermoid-2 cell proliferation. *Head Neck*. 2017;39(4):656–661. doi:10.1002/hed.24648
37. Wang Q, Li C, Ren T, et al. Poly(vinyl methyl ether/maleic anhydride)-doped PEG-PLA nanoparticles for oral paclitaxel delivery to improve bioadhesive efficiency. *Mol Pharm*. 2017;14(10):3598–3608. doi:10.1021/acs.molpharmaceut.7b00612
38. Liu J, Cheng H, Han L, et al. Synergistic combination therapy of lung cancer using paclitaxel- and triptolide-coloaded lipid-polymer hybrid nanoparticles. *Drug Des Devel Ther*. 2018;12:3199–3209. doi:10.2147/DDDT.S172199
39. Joshi MD, Muller RH. Lipid nanoparticles for parenteral delivery of actives. *Eur J Pharm Biopharm*. 2009;71(2):161–172. doi:10.1016/j.ejpb.2008.09.003
40. Bialecka M. [The effect of bioflavonoids and lecithin on the course of experimental atherosclerosis in rabbits]. *Ann Acad Med Stetin*. 1997;43:41–56. Polish.
41. Wu L, Ding J. In vitro degradation of three-dimensional porous poly (D,L-lactide-co-glycolide) scaffolds for tissue engineering. *Biomaterials*. 2004;25(27):5821–5830. doi:10.1016/j.biomaterials.2004.01.038
42. Rezazadeh M, Emami J, Hassanzadeh F, Sadeghi H, Rostami M, Mohammadkhani H. Targeted nanostructured lipid carriers for delivery of paclitaxel to cancer cells: preparation, characterization, and cell toxicity. *Curr Drug Deliv*. 2017;14(8):1189–1200. doi:10.2174/1567201814666170503143646
43. Zhao C, Fan T, Yang Y, et al. Preparation, macrophages targeting delivery and anti-inflammatory study of pentapeptide grafted nanostructured lipid carriers. *Int J Pharm*. 2013;450(1–2):11–20. doi:10.1016/j.ijpharm.2013.04.030
44. Zhao C, Liu Y, Fan T, et al. A novel strategy for encapsulating poorly soluble drug into nanostructured lipid carriers for intravenous administration. *Pharm Dev Technol*. 2012;17(4):443–456. doi:10.3109/10837450.2010.546411
45. Jian Y, Bu W, Chu J, et al. Preparation and characterization of gastric cancer vasculature targeted peptide GX1 mediatednanostructured lipid carriers loaded with paclitaxel. *Chinese J New Drugs*. 2018;27(18):54–61.
46. Chen C, Fan T, Jin Y, et al. Orally delivered salmon calcitonin-loaded solid lipid nanoparticles prepared by micelle-double emulsion method via the combined use of different solid lipids. *Nanomedicine*. 2013;8(7):1085–1100. doi:10.2217/nnm.12.141
47. Accardo A, Mannucci S, Nicolato E, et al. Easy formulation of liposomal doxorubicin modified with a bombesin peptide analogue for selective targeting of GRP receptors overexpressed by cancer cells. *Drug Deliv Transl Res*. 2019;9(1):215–226. doi:10.1007/s13346-018-00606-x
48. Ni YJ, Lu J, Zhou HM. Propofol suppresses proliferation, migration and invasion of gastric cancer cells via regulating miR-29/MMP-2 axis. *Eur Rev Med Pharmacol Sci*. 2019;23(19):8606–8615. doi:10.26355/eurrev_201910_19177
49. Wang Z, Yu K, Hu Y, et al. Schisantherin A induces cell apoptosis through ROS/JNK signaling pathway in human gastric cancer cells. *Biochem Pharmacol*. 2019;113673.
50. Chen B, Cao S, Zhang Y, et al. A novel peptide (GX1) homing to gastric cancer vasculature inhibits angiogenesis and cooperates with TNF alpha in anti-tumor therapy. *BMC Cell Biol*. 2009;10:63. doi:10.1186/1471-2121-10-63
51. Zhang J, Zhang P, Zou Q, et al. Co-delivery of gemcitabine and paclitaxel in cRGD-modified long circulating nanoparticles with asymmetric lipid layers for breast cancer treatment. *Molecules*. 2018;23(11).
52. Kukowska-Latallo JF, Candido KA, Cao Z, et al. Nanoparticle targeting of anticancer drug improves therapeutic response in animal model of human epithelial cancer. *Cancer Res*. 2005;65(12):5317–5324. doi:10.1158/0008-5472.CAN-04-3921

Drug Design, Development and Therapy

Dovepress

Publish your work in this journal

Drug Design, Development and Therapy is an international, peer-reviewed open-access journal that spans the spectrum of drug design and development through to clinical applications. Clinical outcomes, patient safety, and programs for the development and effective, safe, and sustained use of medicines are a feature of the journal, which has also been accepted for indexing on PubMed Central. The manuscript management system is completely online and includes a very quick and fair peer-review system, which is all easy to use. Visit http://www.dovepress.com/testimonials.php to read real quotes from published authors.

Submit your manuscript here: https://www.dovepress.com/drug-design-development-and-therapy-journal